Dark aerobic sulfide oxidation by anoxygenic phototrophs in anoxic waters

Jasmine S. Berg[1,2]*, Petra Pjevac[3], Tobias Sommer[4], Caroline R.T. Buckner[1], Miriam Philippi[1], Philipp F. Hach[1], Manuel Liebeke[1], Moritz Holtappels[5], Francesco Danza[6,7], Mauro Tonolla[6,7], Anupam Sengupta[8,9], Carsten J. Schubert[4], Jana Milucka[1], Marcel M.M. Kuypers[1]

[1]Department of Biogeochemistry, Max Planck Institute for Marine Microbiology, 28359 Bremen, Germany
[2]Institut de Minéralogie, Physique des Matériaux et Cosmochimie, Université Pierre et Marie Curie, CNRS UMR 7590, 4 Place Jussieu, 75252 Paris Cedex 05, France
[3]Division of Microbial Ecology, Department of Microbiology and Ecosystem Science, University of Vienna, 1090 Vienna, Austria
[4]Eawag, Swiss Federal Institute of Aquatic Science and Technology, Kastanienbaum, Switzerland
[5]Alfred-Wegener-Institut, Helmholtz-Zentrum für Polar- und Meeresforschung, Am Alten Hafen 26, 27568 Bremerhaven, Germany
[6]Laboratory of Applied Microbiology (LMA), Department for Environmental Constructions and Design (DACD), University of Applied Sciences and Arts of Southern Switzerland (SUPSI), via Mirasole 22a, 6500 Bellinzona, Switzerland
[7]Microbiology Unit, Department of Botany and Plant Biology, University of Geneva, 1211 Geneva, Switzerland
[8]Physics and Materials Science Research Unit, University of Luxembourg, 162 A, Avenue de la Faencerie, L-1511 Luxembourg City, Luxembourg
[9]Institute for Environmental Engineering, Department of Civil, Environmental and Geomatic Engineering, ETH Zurich, 8093 Zurich, Switzerland.

*corresponding author: Jasmine.Berg@mnhn.fr

ORIGINALITY-SIGNIFICANCE STATEMENT

This study reveals that dark aerobic sulfide oxidation within an anoxic layer dominated by anoxygenic phototrophic bacteria in the stratified water column of Lake Cadagno is to a large extent carried out by the anoxygenic phototrophic bacterium *Chromatium okenii*. Our findings imply that aerobic metabolisms may be more prevalent in anoxic zones than previously thought. We also present an environmental metagenome-assembled genome of *Chr. okenii* which is the first genome sequence for the genus *Chromatium* and reveals new interesting physiological features of this environmentally relevant organism, including its capacity for aerobic respiration.

SUMMARY

Anoxygenic phototrophic sulfide oxidation by green and purple sulfur bacteria (PSB) plays a key role in sulfide removal from anoxic shallow sediments and stratified waters. Although some PSB can also oxidize sulfide with nitrate and oxygen, little is known about the prevalence of this chemolithotrophic lifestyle in the environment. In this study, we investigated the role of these phototrophs in light-independent sulfide removal in the chemocline of Lake Cadagno. Our temporally resolved, high-resolution chemical profiles indicated that dark sulfide oxidation was coupled to high oxygen consumption rates of ~9 µM $O_2 \cdot h^{-1}$. Single-cell analyses of lake water incubated with $^{13}CO_2$ in the dark revealed that *Chr. okenii* was to a large extent responsible for aerobic sulfide oxidation and it accounted for up to 40 % of total dark carbon fixation. The genome of *Chr. okenii* reconstructed from the Lake Cadagno metagenome confirms its capacity for microaerophilic growth and provides further insights into its metabolic capabilities. Moreover, our genomic and single-cell data indicated that other PSB grow microaerobically in these apparently anoxic waters. Altogether, our observations suggest that aerobic respiration

may not only play an underappreciated role in anoxic environments, but also that organisms typically considered strict anaerobes may be involved.

INTRODUCTION

Anoxygenic phototrophic bacteria oxidizing sulfide and fixing CO_2 with sunlight play an important role in the carbon and sulfur cycles of sulfidic, shallow sediments and stratified water columns. Phototrophic sulfur bacteria, for example, are believed to be responsible for 20-85% of the total daily carbon fixation in anoxic lakes (summarized in Cohen *et al.,* 1977). This primary production is so important that it can control the bulk C-isotope fractionation in the water column, generating isotopic signatures that are transported and preserved in sediments (Posth *et al.,* 2017). Biomass from anoxygenic phototrophs both feeds grazing zooplankton in overlying oxic waters (Sorokin 1966) and drives sulfate reduction in anoxic waters below (Pfennig 1975). The phototrophic sulfur bacteria also remove toxic sulfide from the water column, enabling aerobic life at the surface while recycling sulfur compounds for sulfate reducers. While their role in sulfide detoxification has primarily been studied in stratified lakes, there are a few examples of marine environments such as the Black Sea (Jørgensen *et al.,* 1991; Overmann *et al*., 1992; Manske *et al*., 2005; Marschall *et al*., 2010) and the Chesapeake Bay (Findlay *et al.,* 2015) where phototrophic sulfur bacteria also significantly impact sulfur cycling.

Anoxygenic phototrophs generally inhabit illuminated, anoxic, reducing environments which has been attributed to the toxicity of oxygen to these bacteria, and to the competition with abiotic reactions involving oxygen for their electron donors. Abiotic sulfide oxidation with oxygen is kinetically hampered and thus extremely slow (on the order of days) in trace-metal poor waters (e.g. Millero 1986; Millero et al 1987; Luther et al 2011). However, the presence of metals such as Fe, and

73 less importantly Mn, has been shown to catalyze the reaction between sulfide and oxygen (Vazquez
74 et al 1989). Nonetheless, sulfide oxidation by microorganisms possessing enzymes which have
75 evolved to overcome these kinetic constraints likely remains the most important sulfide removal
76 process in most environments (Luther et al. 2011).

77 In fact, some anoxygenic phototrophs have evolved the capacity for chemotrophic growth
78 under microoxic conditions. Whereas the green sulfur bacteria (GSB) of the *Chlorobiaceae*
79 family are considered strict anaerobes, members of the *Proteobacteria* collectively known as
80 the purple sulfur bacteria (PSB) can be facultatively microaerobic (e.g. Kampf and Pfennig, 1980;
81 de Witt and Van Gemerden, 1990). Both the GSB and PSB are well adapted to fluctuating
82 environmental conditions, synthesizing and accumulating storage compounds during periods of
83 substrate/nutrient excess. The anoxygenic phototrophs are known to store zero-valent sulfur
84 (S^0), polyphosphate, glycogen, and in the case of the PSB alone, poly-3-hydroxyalkanoates (PHA)
85 (Mas and Van Gemerden, 1995). The macromolecular structure and metabolism of these
86 compounds have been intensely studied in laboratory pure cultures in order to understand
87 conditions leading to their accumulation and breakdown. It has been suggested that glycogen
88 may play a role in energy generation under dark conditions based on observations that cultured
89 *Chromatium* sp. utilize glycogen to reduce stored sulfur, yielding sulfide and PHA (Van
90 Gemerden, 1968).

91 Here we investigated the role of anoxygenic phototrophic bacteria in dark sulfur cycling
92 processes in Lake Cadagno, a permanently stratified lake with high sulfate concentrations of up
93 to 1-2 mM in the monimolimnion. Microbial reduction of sulfate produces large amounts of
94 sulfide in the anoxic bottom waters (up to ~300 µM) and sediments (>500 µM) which support

95 dense populations of GSB and PSB in the photic zone. These bacteria heavily influence the
96 chemistry of the lake, forming chemocline of 1-2 meters in thickness where sulfide and oxygen
97 remain mostly non-detectable. The PSB *Chromatium okenii* is by far the most active of these
98 bacteria, having been shown to play a disproportionately large role in inorganic carbon and
99 ammonium assimilation despite their low abundances (<1% of total cell numbers) in the
100 chemocline (Musat *et al.,* 2008; Posth *et al.,* 2017). In addition to their important contribution
101 to light-driven sulfide oxidation, previous studies have shown that the anoxygenic phototrophic
102 bacteria of Lake Cadagno remain active in the dark (Musat *et al.,* 2008; Halm *et al.,* 2009; Storelli
103 *et al.,* 2013). However, their mechanism of energy generation in the absence of light is not yet
104 clear. We therefore combined high-resolution biogeochemical profiling with metagenomic
105 analyses to gain an overview of possible light-independent metabolic processes impacting the
106 sulfur biogeochemistry of Lake Cadagno. In addition to providing insights into the metabolism of
107 anoxygenic phototrophic bacteria *in situ*, we present a model to explain the mechanism of dark
108 sulfide oxidation in the chemocline of this meromictic lake.

109 **RESULTS & DISCUSSION**

110 ***Biogeochemistry of Lake Cadagno***

111 Lake Cadagno is characterized by an oxic mixolimnion and a sulfidic monimolimnion spatially
112 separated from each other by a chemocline (defined by bold contour lines in Fig. 1A) free of
113 detectable oxygen (detection limit 50-100 nM) and containing very little sulfide (0-5 µM). In
114 August 2015, oxygen disappeared just above the chemocline close to 12 m depth. The daytime
115 increase in oxygen concentrations between 11-12 m depth denotes net photosynthesis and the

116 nighttime decrease denotes net respiration (Fig. 1A). The permanent absence of oxygen in the
117 chemocline indicated that oxygen was consumed both in the day and the night.

118 Steep gradients of sulfide diffusing into the chemocline varied independently of light-dark
119 periods and the total sulfide concentration in the chemocline did not exceed 5 µM at any time
120 point. Because the lake is meromictic, these stratified conditions were also present during other
121 sampling years (see Fig. S2 for 2013 and 2014 profiles). In 2015, the 0.5-1 m wide chemocline
122 was located around 11-12 m depth, with the exact location varying over the day most likely due
123 to the action of internal waves (Egli *et al.,* 1998). In previous years, the chemocline was up to 2
124 m wide (Fig. S2) and remained completely sulfide-free in the dark. Conservative properties such
125 as temperature and conductivity were constant throughout the chemocline in all years sampled
126 (Fig. S1&2) indicating mixing of this zone (Sommer *et al.,* 2017). Flat conductivity profiles
127 revealed stronger mixing of the chemocline in 2013 and 2014 (Fig. S2) than in 2015 (Fig. S1)
128 when the region of constant conductivity was reduced or absent.

129 *Chr. okenii* was the most significant microorganism in the chemocline both in terms of biomass,
130 accounting for ~60-80% of total microbial biovolume (Sommer *et al.* 2017), and activity,
131 accounting for 30-40% of inorganic carbon fixation (Fig. S3). The cell abundances of *Chr. okenii*
132 in the Lake Cadagno chemocline were enumerated by flow cytometry during 2 daily cycles (Fig.
133 1B). Higher densities of *Chr. okenii* were found in 2014 ($10^6 \cdot ml^{-1}$) than in 2015 ($10^5 \cdot ml^{-1}$). *Chr.*
134 *okenii* is highly motile, swimming at speeds of ~27 $\mu m \cdot s^{-1}$ and has been hypothesized to drive
135 the convection and mixing of the chemocline (Wüest, 1994; Sommer *et al.,* 2017). *Chromatium*
136 are known to migrate between gradients of sulfide, light, and oxygen by photo- and chemotaxis
137 (Pfennig *et al.,* 1968). We observed that *Chr. okenii* were positioned between oxygen and sulfide

138 gradients, regardless of changes in depth or light availability (Fig. 1A,B). The hourly variations in
139 cell numbers were likely the result of their heterogeneous distribution across the chemocline as
140 *Chr. okenii* can swim in a horizontal direction or be displaced by compression of the water
141 masses by internal waves (Egli et al., 1998). Other anoxygenic phototrophs that have been
142 consistently detected in the chemocline include the PSB *Lamprocystis, Thiocystis* and
143 *Thiodictyon* and several GSB of the genus *Chlorobium* (Tonolla *et al.,* 1999, 2004, 2005).
144 Together these bacteria constituted the majority of the total phototrophic cells ($10^6 \cdot ml^{-1}$) in
145 2015, but they are considerably smaller in size (and thus proportion of total biovolume) than
146 *Chr. okenii*.

147 The oxidation of sulfide by these anoxygenic phototrophs proceeds via the formation of S^0 as an
148 obligate intermediate (Mas and Van Gemerden, 1995). This S^0 was measured as particulate
149 sulfur on 0.7 µm filters and may comprise S^0 stored intracellularly by PSB and S^0 adhering
150 extracellularly to GSB. The highest concentrations of S^0 (up to 45 µM; 1C) were measured in the
151 middle of the chemocline. It is likely that this S^0 was present in the form of both elemental S and
152 polysulfides formed by the reaction of free sulfide with intra- and extracellular S^0, as has
153 previously been suggested in other euxinic lakes (Overmann, 1997). Our analytical method for
154 total S^0 did not distinguish between different forms of S^0 such as cyclooctasulfur and
155 polysulfides. However, we could confirm the presence of polysulfides inside live *Chr. okenii* cells
156 in environmental samples using Raman spectroscopy. The Raman spectrum of a sulfur inclusion
157 from *Chr. okenii* exhibited two weak peaks at 152 and 218 and a prominent peak at 462 cm^{-1}
158 (Fig. S4) which is characteristic of linear polysulfide species (Janz *et al.,* 1976). The Raman peak
159 at ~2900 cm^{-1} corresponds to the CH_2 and CH_3 stretching vibrations (Socrates, 2004), and its co-

160 occurrence with polysulfide peaks support the theory that the sulfur chains in these purple
161 sulfur bacteria are terminated by organic end groups as reported previously (Prange *et al.,*
162 1999).

163 Over two diurnal cycles, the S^0 inventory (Fig. S5A), or the total amount of particulate S^0 in the
164 chemocline, was much lower than expected from the sulfide gradients and corresponding
165 sulfide fluxes (discussed below), suggesting that stored S^0 served only as a transient
166 intermediate and was rapidly oxidized to sulfate. No day-night trends in S^0 accumulation were
167 apparent in the chemocline. Nevertheless, the increase in the S^0 inventory at several time points
168 during the night was indicative of dark sulfide oxidation.

169 In culture, *Chromatium* spp. are known to store carbon compounds like glycogen and
170 polyhydroxyalkanoates (PHAs) which have been proposed to be involved in dark sulfur
171 metabolism (Mas and van Gemerden, 1995). We therefore quantified glycogen and PHA
172 abundance in biomass samples from one day/night profile of the chemocline (Fig. 2A&B). We
173 could not detect any PHA, but the presence of glycogen during the day and night coincided with
174 *Chr. okenii* cell numbers (Fig. 2A&B). This is consistent with previous reports of glycogen storage
175 and an absence of PHA in natural populations of *Chr. okenii* (Del Don *et al.,* 1994). While the
176 highest potential cellular glycogen content ($2.38 \cdot 10^{-6}$ µg/cell) was found at the top of the
177 chemocline during the day, we observed little change in the cellular glycogen content between
178 day and night (Fig. S6). Average potential cellular glycogen decreased from $5.50 \cdot 10^{-7}$ µg/cell
179 during the day to $5.33 \cdot 10^{-7}$ µg/cell during the night, which represents a 3% reduction in cellular
180 glycogen reserves. *Chr. okenii* in Lake Cadagno were previously reported to decrease their
181 glycogen reserves by 50 % in the dark (Del Don *et al.,* 1994), but this may have been a result of

182 undersampling as our time- and depth-resolved biogeochemical profiles revealed light-dark
183 independent variations in *Chr. okenii* cell numbers and glycogen concentrations. While it has
184 been demonstrated that *Chromatium* sp. in pure cultures obtain energy from the reduction of S^0
185 with glycogen in the dark (Van Gemerden, 1968), we could not confirm this observation for *Chr.*
186 *okenii in situ.* From our data, we conclude that storage compounds did not play a significant role
187 in the dark respiratory metabolism of *Chr. okenii* in the Lake Cadagno chemocline.

188 Sulfate was measured as the end product of sulfide oxidation, but due to the high (1-2 mM)
189 background sulfate concentrations, the comparably small concentration changes resulting from
190 sulfide oxidation processes were non-detectable. To identify regions of sulfate production in
191 and around the chemocline, we therefore determined deviations from the sulfate-conductivity
192 mixing line drawn for each profile (see Fig. S7 for details). Strong mixing of the chemocline is
193 expected to produce a linear relationship between sulfate and conductivity, and large
194 digressions from this best-fit line indicated that sulfate was produced faster than the rate of
195 mixing. The expected sulfate concentration could be extrapolated based on measured
196 conductivity, and then subtracted from the measured sulfate concentration to give excess
197 sulfate:

198 $$\text{measured } [SO_4^{2-}] - \text{expected } [SO_4^{2-}] = \text{excess } [SO_4^{2-}]$$

199 This excess sulfate was attributed to biological sulfate production, as abiotic sulfide oxidation
200 has been shown to produce mainly S^0 and thiosulfate both in laboratory solutions (Chen and
201 Morris 1972; Gourmelon et al 1977) and in similarly stratified natural environments (Zopfi et al
202 2001; Ma et al 2006). Biogenic sulfate profiles from 2015 plotted over two diurnal cycles

203 exhibited a peak at the top of the chemocline in the region of oxygen depletion (Fig. 1D).
204 Interestingly, sulfate production was observed during the night and the overlap of excess sulfate
205 and oxygen in these profiles indicated that sulfide may be oxidized aerobically. Daytime sulfate
206 production in 2014 was related to photosynthetically active radiation (PAR) intensity (Fig. S2),
207 suggesting that sulfide and S^0 could either have been oxidized aerobically within the chemocline
208 using *in situ*-produced oxygen (Milucka *et al.,* 2015) or phototrophically. The comparatively
209 broad biogenic sulfate peak in the 2014 night profile likely reflects the broader vertical
210 distribution of the *Chr. okenii* population (Fig. S2).

211 The sulfate excess in the chemocline is not expected to be affected by sulfate reduction as no
212 sulfate reduction was detected within the chemocline in 2014 or 2015. The sulfate reduction
213 rates measured in the sulfidic zone 1 m below the chemocline were about 235 $nM \cdot d^{-1}$ and 375
214 $nM \cdot d^{-1}$ in 2014 and 2015, respectively.

215 To quantify biological sulfide consumption over time, we calculated the total sulfide flux into
216 the chemocline (Fig. S5B). Assuming that phototrophic sulfide oxidation ceases in the dark,
217 upwards-diffusing sulfide should accumulate in the chemocline at night. The expected sulfide
218 accumulation was calculated based on fluxes into the layer over a 10-h night period and
219 compared to the actual sulfide concentration observed in the layer. From an average sulfide flux
220 $F = 0.15\ \mu m \cdot cm^{-2} h^{-1}$ (Fig. S5B), into a well-mixed layer of thickness $H = 1$ m over $t = 10$ hours, the
221 resulting sulfide concentration $C = F*t/H$ should be about 15 µM in the chemocline. However,
222 the average sulfide measured in the layer did not exceed 3 µM (Fig. 1A), or five times less than
223 expected, indicating that sulfide is consumed.

We therefore partitioned the total sulfide flux into two fractions: the flux of biologically consumed sulfide and the flux of residual sulfide in the chemocline. First, the amount of residual sulfide was calculated at each sampling time point by integrating sulfide concentrations within the mixed layer (Fig. S5C). The rate of sulfide accumulation was then calculated for each 4-h sampling interval and subtracted from the total sulfide flux to give the biologically consumed sulfide flux. The flux of sulfide consumed in the dark was in the same range as in the day (0.03 to 0.22 $\mu mol \cdot cm^{-2} h^{-1}$) and the residual sulfide flux was very small in comparison (Fig. 2C). The observed variations did not correlate with day-night cycles and the changes of sulfide gradients could have been induced by internal waves, as mentioned above. Together, this indicates that sulfide oxidation continued in the dark and seemed to be related to the total sulfide flux (Fig. S5 B) rather than the presence of sunlight. For comparison, the upwards flux of sulfide in previous years was slightly lower, or 0.011-0.024 $\mu mol \cdot cm^{-2} h^{-1}$ in 2013 and 0.032-0.072 $\mu mol \cdot cm^{-2} h^{-1}$ in 2014.

It was not possible to calculate S^0 fluxes in Lake Cadagno because S^0 is actively transported by the motile purple sulfur bacteria during chemo- and phototaxis (Pfennig *et al.,* 1968) independent of diffusive processes. The total (upwards and downwards) biogenic sulfate flux (Fig. S5 D) in this region was roughly equivalent to the sulfide flux and followed a similar trend.

Overall, our high-resolution profiles revealed that sulfide in Lake Cadagno was consumed during the day and night, but only light-dependent sulfide oxidation has thus far been recognized as a major sulfide-removing process in the lake. In the absence of light, it is also possible that alternative electron acceptors such as NO_x^-, $Fe^{(III)}$, $Mn^{(IV)}$, or O_2 play a role in sulfide oxidation. Nitrate and nitrite concentrations in the Lake Cadagno chemocline are negligible (Halm *et al.,*

2009; Milucka *et al.,* 2015). High fluxes of reduced, dissolved metals (0.027 µmol $Fe \cdot cm^{-2} \cdot d^{-1}$ and Mn 0.049 µmol $Mn \cdot cm^{-2} \cdot d^{-1}$) suggest that Fe- and Mn-oxides are rapidly reduced by microorganisms or abiotically by sulfide in the chemocline (Berg *et al.,* 2016), but re-oxidation of Fe and Mn would ultimately depend on oxygen in the dark. We therefore considered oxygen as the principal direct (or indirect) oxidant responsible for observed dark sulfide oxidation.

The oxygen flux into the chemocline varied slightly between 0.022-0.071 $\mu mol \cdot cm^{-2} h^{-1}$ over the period of 48 h (Fig. 2D). Oxygen fluxes measured in 2013 and 2014 were in the same range, or 0.013-0.048 $\mu mol \cdot cm^{-2} h^{-1}$ and 0.037-0.073 $\mu mol \cdot cm^{-2} h^{-1}$, respectively.

Sulfide oxidation can occur in two steps:

(1) $O_2 + 2HS^- + 2H^+ \rightarrow 2S^0 + 2H_2O$

(2) $2S^0 + 3O_2 + H_2O \rightarrow 4H^+ + 2SO_4^{2-}$

Assuming that all sulfide is eventually oxidized to sulfate, we related oxygen fluxes to sulfide consumption using the 2:1 stoichiometry for complete aerobic sulfide oxidation:

(3) $2O_2 + HS^- \rightarrow 1H^+ + SO_4^{2-}$

Calculated oxygen fluxes in 2013 and 2014 were sufficient to account for all the sulfide oxidized in the dark. In 2015, aerobic sulfide respiration could account for up to 10-50% of sulfide oxidized during the day and 5-45% of sulfide oxidized during the night (Fig. 2D). During the day, the remainder of sulfide oxidation could be attributed to anoxygenic photosynthesis and/or aerobic sulfide oxidation fueled by *in situ* oxygen production by photosynthetic algae. At several time points in the dark, however, we could not explain the disappearance of roughly 60-90% of

upwards-diffusing sulfide. We hypothesize that the missing oxygen is supplied laterally from the turbulent transport initiated by internal wave breaking at the lake boundaries. The convection within the chemocline may be key to the transport of oxygen and sulfide to aerobic sulfide-oxidizing bacteria in the chemocline. A weakening of the mixing regime was observed in August 2015 (Sommer *et al.,* 2017) which may have signified a slowed transport of electron acceptors, thus contributing to the accumulation of sulfide in the chemocline.

To determine potential O_2 consumption rates in the Lake Cadagno chemocline, we performed incubation experiments with chemocline water by sequentially injecting dissolved O_2 and H_2S and monitoring O_2 concentrations online (Fig. S8). Background rates of O_2 consumption prior to H_2S addition were 0.55 - 0.57 $\mu M \cdot h^{-1}$ (Fig. S8 B). Within 5 minutes of H_2S addition, the O_2 consumption rate increased 4- to 5-fold and remained high for 15-30 minutes. The response of the H_2S addition was highly reproducible, resulting in mean rates of 8.7 ± 1.9 $\mu M\ O_2 \cdot h^{-1}$ for five consecutive additions (Fig. S8 B). These potential aerobic respiration rates were well within the range of the volumetric oxygen consumption rates (4.4-14.2 $\mu M\ O_2 \cdot h^{-1}$) determined from *in situ* fluxes over a chemocline of 0.5 m thickness.

For each injection of 1.6 µM H_2S, O_2 concentrations fell by 1.5 to 2.5 µM which is equivalent to a stoichiometry of O_2:H_2S between 1:1 and 2:1. This suggests a combination of sulfide oxidation to sulfur and to sulfate (equations 1 and 3). Based on the experimental oxygen consumption rate, we calculated the most conservative sulfide oxidation rate (using a 2:1 ratio) to be 4.35 µM $H_2S \cdot h^{-1}$. These rates are much higher than would be expected from abiotic sulfide oxidation alone (Millero 1986; et al. Millero 1987) implying that microorganisms play a key role in aerobic sulfide oxidation in Lake Cadagno.

288 ***Dark activity of Chr. okenii in Lake Cadagno***

289 While the sulfide-oxidizing *Chr. okenii* is one of the most active microorganisms in the Lake
290 Cadagno chemocline in terms of C-fixation in the light (Musat et al. 2008; Fig. S3), its metabolic
291 activity and contribution to sulfide removal in the dark has not yet been investigated. The
292 capacity for microaerophilic respiration is known for a few PSB, and it is therefore possible that
293 *Chr. okenii* grows chemoautotrophically on oxygen and sulfide in the absence of light. To test
294 this, we incubated Lake Cadagno chemocline water with added sulfide and $^{13}CO_2$ in the dark
295 under anoxic, low microoxic, and medium microoxic conditions and compared the C-fixation
296 activity of single *Chr. okenii* cells to that under light conditions. In order to mimic the diffusive
297 flux of O_2 in the lake, air was injected into the headspace of the microoxic incubations to
298 achieve expected concentrations of 5 µM and 15 µM dissolved O_2 in the low and medium
299 incubations, respectively. Although bottles were shaken at the start of the incubation to
300 equilibrate the water and headspace and then stirred constantly to enhance diffusion of O_2 into
301 the water, dissolved O_2 concentrations dropped rapidly within the first hour of incubation (Fig.
302 S9) at the same rate (8 µM $O_2 \cdot h^{-1}$) observed in our experimental rate measurements above. For
303 the remainder of the incubation, dissolved O_2 remained below 15 % of the targeted
304 concentrations, most likely because O_2 consumption outpaced diffusion resulting in O_2
305 concentrations close to those observed *in situ*.

306 The incorporation of $^{13}CO_2$ into *Chr. okenii* cells under dark, anoxic conditions was only slightly
307 above background (Fig. 3A). The mean growth rate of 0.009 ± 0.007 d^{-1} could be attributed to
308 trace oxygen contamination or to fermentation of carbon storage compounds as reported by
309 Van Gemerden (1968). A few small rod-shaped cells were also enriched in ^{13}C and were likely

310 sulfur-disproportionating bacteria such as *Desulfocapsa* and *Desulfobulbus* which have
311 previously been identified in Lake Cadagno (Tonolla et al. 2000; Peduzzi et al 2003). In the
312 microoxic incubations, dark C-fixation activity of *Chr. okenii* increased proportionally with the
313 amount of O_2 added (Fig 3B&C) confirming that these bacteria obtained energy from aerobic
314 respiration. The mean growth rate at an expected concentration of 15 µM O_2 (0.082 ± 0.021 $d^{-}1$)
315 was about three times higher than at an expected concentration of 5 µM O_2 (0.025 ± 0.008 d^{-1}).
316 Based on these growth rates and total cell abundances, we could estimate that *Chr. okenii*
317 accounted for 31-42 % of the dark C-assimilation measured by bulk analyses (Fig. S3).

318 Clusters of cells reminiscent of the PSB *Thiodictyon* as well as a few other bacterial filaments
319 and rod-shaped cells that were most likely aerobic, sulfide-oxidizing bacteria were also highly
320 enriched in ^{13}C (Fig 3B&C). This suggests that the capacity for aerobic respiration is
321 taxonomically widespread in the anoxic chemocline.

322 Surprisingly, *Chr. okenii* growth rates in the light (0.100 ± 0.033) were only slightly higher than
323 under microoxic conditions (Fig 3E) and their activity represented about 25 % of the total C-
324 assimilation (Fig. S3). Since this incubation was performed over a full light-dark cycle, it is also
325 possible that activity was restricted to the 13-h light period, which would yield a higher hourly
326 growth rate. While it is difficult to disentangle phototrophic from chemoautotrophic carbon
327 fixation in this case, the presence of abundant associations of *Chr. okenii* cells with eukaryotic
328 algae (Fig. 3D) indicates that these PSB can also thrive off local light-driven O_2 production. We
329 could show that algae were photosynthetically active via the incorporation of $^{13}CO_2$ into the
330 eukaryotic cells (Fig. S10). Diffusion of O_2 to attached *Chr. okenii* cells may have stimulated
331 chemoautotrophic growth as they were also highly enriched in ^{13}C.

332 *Chr. okenii* use energy from aerobic respiration not only for anabolic processes but for motility
333 as well. We could confirm that *Chr. okenii* are highly motile both in the day and the night by
334 performing dark field video microscopy (see Movie S1 in Supplementary Materials) of
335 environmental samples obtained during the night and monitored in a dark room to avoid light-
336 induced artefacts. Although the average night time swimming speed of *Chr. okenii* (9.9 µm s^{-1};
337 see Fig. S11) was a third of the day time swimming speed (27 µm s^{-1}; Sommer et al. 2017), it is
338 clear that *Chr. okenii* remains motile even under dark conditions. This motility may in fact be key
339 to bridging spatially separated gradients of oxygen and sulfide on which they grow.

340 ***Metagenomic insights into the* Chr. okenii *population in Lake Cadagno***

341 To assess the genomic potential for light-independent, aerobic sulfide oxidation by *Chr. okenii* in
342 Lake Cadagno, we sequenced two metagenomes, one from the chemocline and one from a
343 phototrophic, sulfide-oxidizing enrichment culture obtained from the lake (Table S1). From a
344 combined metagenomics assembly, we reconstructed a high quality (90% complete, <1%
345 contaminated) metagenome-assembled genome (MAG) of a PSB highly abundant in the sulfur-
346 oxidizing enrichment culture (Fig. S12). The recovered MAG had a low average nucleotide
347 identity ANI (<70%) to any sequenced *Chromatiaceae* genomes (data not shown). However, it
348 encoded an rRNA operon, including a complete 16S rRNA gene with 99% sequence identity to
349 the 16S rRNA gene of *Chr. okenii* (Imhoff *et al.,* 1998; Tonolla *et al.*, 1999), and thus likely
350 represents a strain of *Chr. okenii* which is the type strain of the genus *Chromatium*. At this time,
351 *Chr. okenii* has not been successfully isolated in pure culture, nor is there any published genome
352 available for this organism.

353 The key metabolic process of *Chr. okenii* in Lake Cadagno is photoautotrophic sulfur oxidation.
354 In accordance, the *Chr. okenii* MAG contained genes encoding for a sulfide : quinone reductase
355 (*sqr*) and the full genomic inventory coding for a reverse-acting dissimilatory sulfite reductase
356 (rDSR) pathway (Fig. 4). The operon structure of the rDSR encoding genes (*dsrABEFHCMKLJOPN*)
357 was identical to the operon structure in the well described PSB model organism *Allochromatium*
358 *vinosum* (Dahl *et al.,* 2005), but no *dsrR* and *dsrS* gene were found. No genes encoding for sulfur
359 oxidation via the SOX pathway, or homologues of sulfur globule proteins (*sgpABC*) typically
360 found in PSB were detected in the draft genome. In line with its phototrophic metabolism, the
361 *Chr. okenii* MAG showed the genomic potential for photosynthesis, with the genes encoding for
362 a light harvesting complex 1 (*pufAB*) and a PSB-type photosynthetic reaction center (*pufLMC*)
363 encoded in a single operon. Furthermore, the full genomic repertoire for a NADP-Me type C4
364 photosynthetic carbon assimilation cycle, and all genes (with exception of *cbbS* encoding for the
365 small subunit of the ribulose-1,5-bisphosphate carboxylase/oxygenase) necessary for CO_2
366 assimilation via the Calvin-Benson-Bassham (CBB) Cycle were present (Fig. 4).

367 Many *Chromatiaceae* can grow chemoautotrophically, respiring oxygen under microoxic
368 conditions (Kämpf and Pfennig, 1980). Cytochrome (Cyt) *c*-containing oxidases (e.g. Cyt *aa3*, Cyt
369 c*bb3*) were not found in the *Chr. okenii* MAG. However, a Cyt *bd* type ubiqinol oxidase, known
370 to function as sulfide-resistant O_2-accepting oxidase in other *Gammaproteobacteria* (Forte *et*
371 *al.,* 2016), was identified (Fig. 4). Further, a plethora of genes related to heme *b* (*gltX*,
372 *hemALBCD*, and *hemH*) and siroheme (*cysG*) synthesis, degradation (a heme oxygenase) and
373 export (ABC-type heme exporter, *ccmABCD*), as well as hemerythrin-like metal binding proteins
374 were encoded. Hemerythrin has been implicated in binding of oxygen for delivery to oxygen-

375 requiring enzymes, for detoxification, or for oxygen sensing in motile, microaerobic prokaryotes
376 (French *et al.,* 2007). The presence of these oxygen-dependent enzymes, as well as a key
377 oxidative stress defense enzyme superoxide dismutase (SOD), support the idea that *Chr. okenii*
378 may be facultatively microaerobic. A complete set of genes for flagellar biosynthesis
379 (*fliDEGHJKLMNOPQRW*, *flgABCDEFGHIK*, *flhAB*) and flagellar motor proteins (*motAB*) confer
380 motility to this bacterium.

381 Several other genes revealed interesting metabolic capacities of *Chr. okenii.* A cytosolic
382 bidirectional [NiFe] type 3d hydrogenase and a nitrogenase were encoded in the MAG (Fig. 4),
383 implicating the potential for involvement of *Chr. okenii* in nitrogen fixation and hydrogen
384 oxidation which has previously been overlooked. Additionally, the *Chr. okenii* MAG encoded a
385 glycogen synthase and a glycogen debranching enzyme, as well as the full genomic repertoire
386 necessary for polyhydroxyalkanoate (PHA) biosynthesis. This is consistent with the detection of
387 glycogen in our biogeochemical profiles of the chemocline. Finally, it is possible that novel
388 terminal oxidases are among the hypothetical genes that could not be assigned any known
389 function.

390 **CONCLUSIONS**

391 It is intriguing that oxygen should play a major role in sulfide oxidation in the ostensibly anoxic
392 chemocline of Lake Cadagno, especially by purple sulfur bacteria generally thought to lead an
393 anaerobic lifestyle. To explain the coupling of oxygen and sulfide consumption in the oxygen-
394 and sulfide-free chemocline of Lake Cadagno, we sketched a diagram of the transport processes
395 likely driving biological activity there (Fig. 5). As described in Sommer *et al.,* (2017), active
396 convection of the chemocline can be driven by the formation of sinking bacterial plumes.

397 Combined with turbulence induced by the breaking of internal waves at the sides of the lake
398 basin, these convective currents may entrain sulfide and oxygen at the boundaries of the
399 chemocline and fuel populations of sulfide-oxidizing *Chr. okenii* there.

400 Sulfur-oxidizing bacteria have previously been reported to bridge distances between pools of
401 electron donors and acceptors by intracellularly storing and transporting S^0 and NO_3^- between
402 redox zones (Fossing *et al.,* 1995; Jørgensen and Gallardo, 1999) and even by transferring
403 electrons along nanowires (Pfeffer *et al.,* 2012), but aerobic sulfide oxidation in Lake Cadagno
404 represents a new mechanism of electron acceptor/donor coupling across large distances. After
405 entrainment into the chemocline, dissolved oxygen and sulfide are consumed so rapidly that
406 they remain below detection limits. The physical and biological processes described here may
407 therefore provide clues to sulfide oxidation in other anoxic environments such as the Black Sea
408 where the mechanism of sulfide removal is not completely understood. Clearly, the biochemical
409 limits to oxygen utilization are far below current definitions of anoxia and demonstrate that
410 aerobic respiration is possible in so-called "anoxic" lacustrine (Milucka *et al.,* 2015) and marine
411 (Garcia-Robledo *et al*., 2017) waters.

412 Although purple sulfur bacteria are generally considered anaerobes, we propose that *Chr. okenii*
413 in the Lake Cadagno chemocline aerobically respire upwards-diffusing sulfide in addition to
414 performing phototrophic sulfide oxidation as previously reported (e.g. Tonolla et al. 1999;
415 Musat et al 2008; Storelli et al. 2013). Our direct evidence for oxygen-driven C-fixation and
416 continued motility of *Chr. okenii* in darkness is also supported by the presence of a potential
417 high-affinity oxidase in the metagenome-assembled genome. In contrast to observations from

418 laboratory cultures, *Chr. okenii* may have a very different metabolism in the environment where
419 high fluxes of substrates rather than absolute substrate concentrations fuel microbial activity.

420 Our nanoSIMS measurements revealed that in addition to *Chr. okenii*, a number of phototrophic
421 and non-phototrophic cells are also highly active under aerobic, sulfide-oxidizing conditions.
422 Based on the diversity of genes encoding for high-O_2 affinity terminal oxidases found in our Lake
423 Cadagno metagenome, it appears that some other purple sulfur bacteria as well as a handful of
424 *Gamma-* and *Epsilonproteobacteria* might aerobically oxidize sulfide (Fig. S13). Interestingly,
425 two species of strictly anaerobic green sulfur bacteria from Lake Cadagno also possessed genes
426 encoding for terminal oxidases, though further study will be required to elucidate the role of
427 these different bacterial populations in chemotrophic sulfide oxidation.

428 **EXPERIMENTAL PROCEDURES**

429 **Sampling**

430 The meromictic Lake Cadagno is situated in the Piora Valley in the Swiss Alps at an altitude of
431 1921 m. Data presented here were collected during field campaigns in September 2013, August
432 2014, June 2015 August 2015, and August 2018. In 2013 and 2014 *in situ* measurements were
433 performed with a profiling ion analyzer (PIA; see Kirf *et al.,* 2014 for description) lowered from a
434 platform anchored at the deepest part of the lake (20.7 m). Conductivity, turbidity, depth
435 (pressure), temperature and pH were measured with a multi-parameter probe (XRX 620, RBR).
436 Dissolved oxygen was recorded online with a type PSt1 normal (detection limit 125 nM) micro-
437 optode and a type TOS7 trace (reliable detection limit 50-100 nM) micro-optode (PreSens). The
438 oxygen sensors were calibrated by parallel Winkler titrations. Water samples for chemical
439 analyses and cell counts were collected with a rosette syringe sampler equipped with twelve 60-

440 ml syringes triggered online at selected depths. Due to a technical failure of the PIA, the 6 AM
441 profile in August 2014 and all subsequent profiles were measured with an SBE 19 plus V2 CTD
442 probe (Sea-Bird Electronics) equipped with sensors for pressure, temperature and conductivity,
443 and with additional sensors for turbidity (WET Labs Eco), oxygen (SBE 43), pH (18-I) and two
444 fluorescence wavelengths (WET Labs ECO-AFL). The detection limit of the SBE 43 oxygen probe
445 was about 1 µmol/l. In parallel with *in situ* measurements, water for chemical analyses was
446 pumped to the surface through Neoprene tubing attached to the CTD and filled into 60-ml
447 syringes (rinsed 2 X with *in situ* water) on board. Two parallel metal plates of diameter ~15 cm
448 attached to the submersed end of the tubing served to channel water horizontally, resulting in
449 more discrete vertical profiling.

450 Water samples in syringes were aliquoted on board immediately after collection. Samples for
451 sulfate analyses were filtered (0.22 µm pore size) directly into sterile Eppendorf vials. Sulfide
452 samples were fixed with Zn-acetate to a final concentration of 0.1 % (w/v). Biomass was
453 concentrated onto GF/F filters (Whatman) and stored at -20°C for analyses of intracellularly
454 stored elemental sulfur and organic carbon compounds. Filtrate (0.22 µm pore size) was also
455 collected and frozen at -20°C for metabolome analysis of dissolved compounds. Water for
456 dissolved inorganic carbon (DIC) analysis was filled into 12-ml Exetainers (Labco Limited) and
457 capped before injecting 100 µl of saturated $HgCl_2$ solution to terminate microbial activity.
458 Biomass samples for determination of background ^{13}C in the particulate organic carbon (POC)
459 were concentrated onto pre-combusted (6 h at 600 °C) GF/F filters. Samples for DNA analysis
460 were collected from the chemocline in August 2014 by concentrating microbial cells on 0.22 µm
461 GTTP-type polycarbonate filters (Millipore) on site and freezing at -20°C until further processing.

462 Additional water for cultivation and motility experiments was pumped directly from the
463 chemocline into 1-L Duran bottles or 250-ml serum bottles and sealed with butyl rubber
464 stoppers without a headspace to maintain anoxic conditions.

465 **Chemical Analyses**

466 Sulfide was measured using the colorimetric method of Cline (1969). Sulfate was measured on a
467 761 Compact ion chromatograph (Metrohm) equipped with a Metrosep A SUPP 5 column.
468 Intracellular sulfur on filters was extracted by sonication in methanol for 15 min in an ice bath.
469 Samples were analyzed on an Acquity H-Class UPLC system (Waters Corporation) with an
470 Acquity UPLC BEH C18 column coupled to a photodiode array (PDA) detector using UPLC-grade
471 methanol as eluent. Data was acquired and processed using the Empower III software.

472 Intracellular glycogen was analyzed following the procedures of the assay kit (MAK016, Sigma
473 Aldrich). Briefly, cells were extracted by scraping them from GF/F filters and homogenizing in
474 200 µL extraction buffer and centrifuged two times to clear the supernatant. The supernatant
475 was analyzed fluorometrically after incubation with enzyme mix and fluorescent peroxidase
476 substrate. Intracellular PHA was analyzed using the protocol from Braunegg *et al.*, (1978).
477 Hydrolyzation of the polymer and conversion to a methyl-ester of the monomeric
478 hydroxyalkanoate fraction was done in acidified alcohol solution (6% H_2SO_4 in methanol) and
479 chloroform under heating (100°C, 2 h). After addition of water and phase separation the organic
480 phase was analyzed with GC-MS (Agilent 7890B GC connected to Agilent 5977A MSD) to detect
481 the methylhydroxyalkanoates using the following settings: Agilent 30 m DB-5-MS column,
482 splitless injection of 1 µl, temperature program was 50°C for 1 min than heating 10°C/min until
483 120°C followed by 45°C/min until 320°C and hold for 5 minutes. Benzoic acid was used as

484 internal standard in each sample and quantification was done with pure polyhydroxybutyrate
485 standard (Sigma Aldrich).
486 Sulfate reduction rates were measured by adding the radiotracer $^{35}SO_4^{2-}$ (5 MBq) to anoxic lake
487 water in 50-ml glass syringes and incubated in the dark. A solution of unlabeled Na_2S was added
488 to a final concentration of ~50 $\mu mol \cdot l^{-1}$ as a background sulfide pool in case of sulfide re-
489 oxidation. At each sampling point, 10 ml of sample was dispensed into 5 ml of 20% (w/v) Zn-
490 acetate. Reduced sulfur species (e.g. sulfur and sulfide as ZnS) were separated out via the
491 chromium distillation method described in Kallmeyer *et al.,* (2004) and the radioactivity per
492 sample was determined via scintillation counting (Packard 2500 TR).
493 **Confocal Raman spectroscopy**
494 In a glove box under 90:10 N_2-CO_2 atmosphere, a drop of fresh sample from the chemocline was
495 mounted between two glass coverslips and sealed with electrical tape to prevent contact with
496 air. A polysulfide solution containing 5.06 g $Na_2S \cdot 9H_2O$ and 5.8 g elemental sulfur per 100 ml
497 H_2O, with a final pH of 9.5 and sulfide concentration of 210 mM, was used as reference.
498 Measurements were conducted with an NTEGRA Spectra confocal spectrometer (NT-MDT)
499 coupled to an inverted Olympus IX71 microscope. The excitation light from a 532-nm solid-state
500 laser was focused on the sample through an Olympus 100X (numerical aperture [NA], 1.3) oil
501 immersion objective. Raman scattered light was collected by an electron-multiplying charge-
502 coupled device (EMCCD) camera (Andor Technology) cooled to -70°C. Spectra were recorded
503 between 0 and 4,500 cm^{-1} with a spectral resolution of 0.2 cm^{-1} and analyzed with the NT-MDT
504 software Nova_Px 3.1.0.0.
505 **Flux Calculations**

Turbulent fluxes (J) of sulfide, sulfur, sulfate, and oxygen at the chemocline were calculated assuming steady state by applying Fick's first law: $J=-D\partial C/\partial x$. For sulfide, sulfate, and oxygen we used the turbulent diffusion coefficient (D) of 1.6×10^{-6} m^2 s^{-1} from (Wüest, 1994) corresponding to turbulence at the Lake Cadagno chemocline boundaries. For sulfur gradients within the well-mixed chemocline the coefficient $D = 1.5 \times 10^{-5}$ m^2 s^{-1} from Wüest (1994) was used. The change in concentration (∂C) was computed for each species over the depths with the steepest gradients. Oxygen and sulfide fluxes were determined for the regions immediately above and below the chemocline, defined as the zone of constant conductivity.**Potential oxygen consumption rate measurements**

Potential O_2 consumption rate measurements were conducted as described in Holtappels et al. (2014). Incubations were performed in 250 ml Winkler bottles using trace oxygen sensor spots (Ø5mm, TROXSP5, Pyroscience) glued to the inner glass wall and read from the outside using a 4-channel fiber-optic oxygen meter (FireStingO2, Pyroscience) recording O_2 concentration every 10 seconds. The glass stopper of the Winkler bottle was pierced with a glass tube (11 cm long, inner diameter 1.5 mm), to allow for pressure compensation due to temperature-induced volume changes and to facilitate the addition of small amounts of reagents. Oxygen transport through this opening was limited by diffusion through a narrow passage over a long distance. Tests with degassed sterile water showed negligible O_2 concentration changes of 3-25 nM·d^{-1} (figures available on request). Water inside the incubation bottles was gently mixed by small glass-coated magnets driven by an adjacent magnetic stirrer. The incubation bottles were placed in a temperature-controlled water bath set to 4.8°C (+/- 0.1°C). A two-point calibration of

527 the trace optode spots was performed by using degassed water to which a known amount of
528 O_2-saturated water was added through the glass tube.

529 Anoxic chemocline water was pumped onboard a sampling platform and distributed directly
530 into incubation vessels via Neoprene tubing, avoiding atmospheric contamination as described
531 above. Bottles were placed immediately into the water bath and incubated in the dark for 18
532 hours. Initial O_2 values were between 6 and 8 µM. Over a period of 12 hours, H_2S was added 5
533 times by injecting up to 300 µl of a 4 mM Na_2S stock solution to a final concentration of 1.6 µM.
534 Between 4-6 ml O_2-saturated lake water from the same depth was periodically added to
535 maintain O_2 concentrations between 5 and 11 µM. O_2 consumption rates were calculated from
536 linear regressions over 10-30 min time intervals.

537 **Stable isotope incubations**

538 250-ml serum bottles containing Lake Cadagno chemocline water collected in August 2018 were
539 bubbled for 10 min with N_2 to remove any contaminant oxygen. Four different incubation
540 conditions were set up to test microbial carbon fixation under the following conditions: no O_2 +
541 dark, no O_2 + light, medium O_2 + dark, and high O_2 + dark. To each of the dark incubations, 50 ml
542 of water was removed and replaced with N_2 gas. Solutions of Na_2S and ^{13}C-DIC were added to
543 final concentrations of 25 µM and 1 mM (36-39 atom %), respectively, except for the light
544 incubation which received 200 µM (8 atom %) ^{13}C-DIC. Volumes of 0.918 ml and 2.8 ml air were
545 added to the dark, aerobic incubations to achieve headspace O_2 concentrations of 129 and 388
546 µM, respectively, resulting in expected dissolved O_2 concentrations of 5 and 15 µM,
547 respectively, at the start of the incubations (Garcia and Gordon, 1992). All bottles were gently

548 shaken for several minutes to equilibrate the water and headspace and then placed in a 10°C
549 water bath in the dark for 18 h, except for the light condition which was incubated separately
550 under natural light, 0.1 – 2 % incident daylight, for a full light-dark cycle. Equilibration with the
551 headspace was enhanced throughout the incubation by stirring with glass-coated magnetic stir-
552 bars at minimum speed.

553 In order to verify the consumption of oxygen, two bottles prepared without ^{13}C-DIC and injected
554 with 0.918 ml and 2.8 ml of air were incubated in parallel with needle optodes (FirestingO2,
555 Pyroscience) immersed in the liquid phase. Dissolved O_2 concentrations were recorded every 3
556 min and are shown in Fig. S9.

557 At the end of the experiment, bottles were sacrificed for analysis of bulk and single-cell ^{13}C
558 uptake. Water for ^{13}C-DIC and ^{13}C-POC was sampled as described above. For nanoSIMS, water
559 samples were fixed with formaldehyde (2 % v/v) overnight at 4°C before filtering onto 0.2 µm
560 Au/Pd-sputtered polycarbonate filters (Millipore) and stored at -20°C until processing.

561 **Mass spectrometry isotope uptake analysis**

562 The labeling % of ^{13}C-DIC was determined by diluting Hg-killed water 1:10 in MilliQ and
563 transferring 3 ml into a 12 ml Exetainer with an N_2 headspace. Samples were then acidified with
564 the addition of ~100 µl concentrated H_3PO_4 so the outgassed $^{13}CO_2$ could be analyzed by cavity
565 ring-down spectroscopy (G2201-i Picarro).

566 The incorporation of ^{13}C from $^{13}CO_2$ into biomass was measured by combustion of the
567 particulate organic carbon fraction on GF/F filters. Filters were decalcified by incubation with
568 37% fuming HCl overnight, dried in an oven at 60°C, and then packed into tin capsules for

569 combustion analysis. The C isotopic composition was determined on an automated elemental
570 analyzer (Thermo Flash EA, 1112 Series) coupled to a Delta Plus XP IRMS (Thermo Finnigan).

571 **Nanometer-scale secondary ion mass-spectrometry**

572 Circular pieces (5-mm diameter) were punched out of the Au/Pd-sputtered filter and regions of
573 interest were marked with a laser micro-dissection microscope (LMD) (DM 6000 B, Leica
574 Microsystems) before analysis with the nanoSIMS 50L (Cameca) at the Max Planck Institute for
575 Marine Microbiology in Bremen, Germany. For each field of view, the sample was pre-sputtered
576 with a primary Cs^+ beam of 300 pA, and then measured by rastering a primary Cs^+ beam with a
577 diameter of < 100 nm and a beam current between 1.0 and 1.5 pA over the area. Secondary ion
578 images of $12C^-$, $13C^-$, $12C14N^-$, $31P^-$ and $32S^-$ were recorded simultaneously using 5 detectors
579 together with the secondary electron (SE) image ranging from 10 x 10 µm to 50 x 50 µm in size
580 and corresponding to an image size of 256 x 256 and 512 x 512 pixels, respectively, using a dwell
581 time of 1 ms per pixel. Up to 60 planes were recorded for each imaged area.

582 Images were processed using the Matlab-based Look@NanoSIMS software (Polerecky *et al.,*
583 2012). Regions of interest (ROIs) were drawn around cells based on the $12C14N^-$ signal overlain
584 on SE images and *Chr. okenii* cells were identified based on morphology, size, and pigmentation
585 in parallel light-microscope images. Cellular ^{13}C atm. % was calculated from $^{13}C/^{12}C$ values of
586 individual ROIs. The background (cell-free polycarbonate filter) ^{13}C content was also evaluated
587 in every field of view for comparison. Growth rates were calculated assuming a linear growth
588 rate where one cell division results in a maximum of ½ the labeling percentage:

589 g = (atm % ^{13}C excess $_{cells}$/ ½ atm % ^{13}C excess $_{tot\ dissolved}$) / t_{hours}

590 Cellular C-uptakes rates were calculated based on the relationship between biovolume and C-
591 content from Verity *et al*., (1992), assuming an average biovolume of spherocylinders cells of 65
592 μm^3 based on direct measurements of 70 *Chr. okenii* cells.

593

594 . **Motility analysis**

595 Water samples containing *Chr. okenii* cells were collected under anoxic conditions from the
596 chemocline during the night, protected from artificial light with aluminum foil, and analyzed
597 immediately on site. Motile cells were transferred via a degassed glass syringe to a sealed
598 rectangular millimetric chamber (dimensions 20 mm × 10 mm × 2 mm) prepared using glass
599 slides separated by a 2-mm thick spacer, which provided an anoxic environment during motility
600 characterization. Experiments were conducted in a dark room, and imaging was performed
601 using the dark field microscopy mode at 25 fps, with the lowest intensity illumination. No
602 transient response was observed right at the start of the imaging, and the swimming velocity
603 remained steady throughout the duration of the measurements. This is in contrast to swimming
604 behavior at higher light intensities where the swimming cells exhibited a positive phototactic
605 response (Sommer *et al*., 2017). We could therefore rule out a light-induced effect on motility at
606 the minimum illumination level used for our measurements. Videos of swimming cells were
607 acquired and subsequently analyzed using the ImageJ Particle Tracker routine to obtain the
608 coordinates of the cells (geometric centers) at each time interval. These were used to calculate
609 the swimming speeds and extract the trajectories of individual cells.

610 **DNA extraction, sequencing, and analysis**

611 Two metagenomes were sequenced: one from the chemocline and one from a phototrophic,
612 sulfide-oxidizing enrichment from the lake. The enrichment culture was obtained by preparing
613 agar-stabilized sulfide-gradient tubes as described in Schwedt et al. (2012) using sterile-filtered
614 Lake Cadagno water amended with vitamins and trace elements as described for cultivation of
615 purple sulfur bacteria (Eichler and Pfennig, 1988). After inoculation with water from the
616 chemocline, cultures were incubated for approximately 3 months in indirect light at 15°C until
617 development of a deep purple color indicative of growth of PSB.

618 DNA was extracted from polycarbonate filters with the Ultra Clean MoBio PowerSoil DNA kit
619 (MoBio Laboratories, Carlsbad, USA) according to the manufacturer's protocol with the
620 following modification: the bead beating step was reduced to 30 sec followed by incubation on
621 ice for 30 sec, repeated 4x. The DNA was gel-purified using SYBR Green I Nucleic Acid Gel Stain
622 (Invitrogen) and the QIAquick Gel Extraction Kit (Qiagen) according to the accompanying
623 protocols. DNA concentration was determined fluorometrically at 260 nm, using the Qubit 2.0
624 Fluorometer and the Qubit dsDNA HS Assay KIT (Invitrogen) and sent to the Max Planck-
625 Genome Centre (Cologne, Germany) for sequencing. The metagenome was sequenced (100 bp
626 paired end reads) by Illumina HiSeq (Illumina Inc., USA) sequencing following a TruSeq library
627 preparation. Metagenomic reads were adapter- and quality-trimmed (phred score 15, bbduk
628 function of the BBMap package, https://sourceforge.net/projects/bbmap/) and paired-end
629 reads were *de novo* assembled with the uneven depth assembler IDBA-UD (Peng *et al.,* 2012).

630 The metagenome assembly was binned based on tetranucleotide frequencies, differential
631 coverage, taxonomic classification, and conserved single-copy gene profiles with the Metawatt
632 binning software (version 3.5.2; Strous *et al*., 2012). The completeness and contamination of the

633 binned MAGs was evaluated with CheckM (Parks et al 2014). The bulk metagenome and the
634 MAG identified as *Chr. okenii* were automatically annotated in IMG (Markowitz et al 2011), and
635 the *Chr. okenii* MAG was manually screened for the presence of genes of interest to this study.
636 Assembled data is available in IMG, under the IMG genome IDs 3300010965 (bulk assembly) and
637 2700988602 (*Chr. okenii* MAG).

638 Cytochrome *c* and quinol oxidase subunit I and the cytochrome *bd* oxidase subunit I proteins
639 were extracted from the metagenome via Pfam motif search (PF00115 and PF01654,
640 respectively), and manually inspected to exclude NO reductase subunit I (NorB) proteins and
641 proteins shorter than 100 aa prior to downstream analysis. A total of 130 out of 178 identified
642 cytochrome *c* and quinol oxidase subunit I proteins and 76 out of 82 recovered cytochrome *bd*
643 oxidase subunit I proteins passed the manual curation step. For phylogenetic tree
644 reconstruction, the manually vetted protein sequences and a selection of reference sequences
645 recovered from NCBI were aligned using MAFFT (Katoh *et al.,* 2002) and IQ-TREE was used to
646 construct the phylogenetic tree with automated best model prediction and a total of 1000
647 bootstrap replicates (Trifinopoulos *et al.,* 2016; Hoang *et al.,* 2017). Thereafter, a selection of
648 sequences closely related to known sulfur oxidizing microorganisms alongside the respective
649 reference sequences were used for reconstruction of the phylogenetic trees presented in Fig.
650 S11. The output files were uploaded to iTOL for visualization (Letunic *et al.,*
651 2016).**ACKGNOWLEDGEMENTS**

652 We are grateful to the 2014 and 2015 Cadagno Field Expedition Teams from EAWAG and MPI
653 Bremen for assistance in the field, and to the Alpine Biology Center Foundation (Switzerland) for
654 use of its research facilities. We would especially like to thank Abiel Kidane and Sten Littman for

help with nanoSIMS measurements as well as Nadine Rujanski, Gabriele Klockgether, and Gaute Lavik for mass spectrometry analyses. Funding was provided by the International Max Planck Research School of Marine Microbiology, the Max Planck Society, and the Deutsche Forschungsgemeinschaft (through the MARUM Center for Marine Environmental Sciences). A.S. was supported by the Human Frontier Science Program (Cross Disciplinary Fellowship, LT000993/2014-C).

662 **REFERENCES**

663 Berg, J.S., Schwedt, A., Kreutzmann, A.-C., Kuypers, M.M., and Milucka, J. (2014) Polysulfides as
664 Intermediates in the Oxidation of Sulfide to Sulfate by Beggiatoa spp. *Applied and Environmental*
665 *Microbiology* **80**: 629-636.

666 Braunegg, G., Sonnleitner, B. Y., and Lafferty, R. M. (1978). A rapid gas chromatographic method for the
667 determination of poly-β-hydroxybutyric acid in microbial biomass. *Applied Microbiology and*
668 *Biotechnology* **6:** 29-37.

669 Chen, K. Y., & Morris, J. C. (1972). Kinetics of oxidation of aqueous sulfide by oxygen. *Environmental*
670 *Science & Technology* **6:** 529-537.

671 Cline, J.D. (1969) Spectrophotometric determination of hydrogen sulfide in natural waters. *Limnology*
672 *and Oceanography* **14**: 454-458.

673 Dahl, C., Engels, S., Pott-Sperling, A. S., Schulte, A., Sander, J., Lübbe, Y., ... and Brune, D. C. (2005). Novel
674 genes of the dsr gene cluster and evidence for close interaction of Dsr proteins during sulfur oxidation in
675 the phototrophic sulfur bacterium *Allochromatium vinosum*. *Journal of Bacteriology* **187**: 1392-1404.

676 Dahl, T.W., Anbar, A.D., Gordon, G.W., Rosing, M.T., Frei, R., and Canfield, D.E. (2010) The behavior of
677 molybdenum and its isotopes across the chemocline and in the sediments of sulfidic Lake Cadagno,
678 Switzerland. *Geochimica et Cosmochimica Acta* **74**: 144-163.

679 De Witt, R., and Van Gemerden, H. (1990) Growth of the phototrophic purple sulfur bacterium
680 Thiocapsaroseopersicina under oxic/anoxic regimens in the light. *FEMS Microbiology Ecology* **6**: 69-76.

681 Del Don, Chr., Hanselmann, K.W., Peduzzi, R., and Bachofen, R. (1994) Biomass composition and
682 methods for the determination of metabolic reserve polymers in phototrophic sulfur bacteria. *Aquatic*
683 *Sciences* **56**: 1-15.

684 Egli, K., Wiggli, M., Klug, J., and Bachofen, R. (1998) Spatial and temporal dynamics of the cell density in a
685 plume of phototrophic microorganisms in their natural environment. *Doc Ist Ital Idrobiol* **63**: 121-126.

686 Eichler, B., & Pfennig, N. (1988). A new purple sulfur bacterium from stratified freshwater lakes,
687 Amoebobacter purpureus sp. nov. *Archives of Microbiology* **149:** 395-400.

688 Findlay, A.J., Bennett, A.J., Hanson, T.E., and Luther, G.W. (2015) Light-dependent sulfide oxidation in the
689 anoxic zone of the Chesapeake Bay can be explained by small populations of phototrophic bacteria.
690 *Applied and Environmental Microbiology* **81**: 7560-7569.

691 Forte, E., Borisov, V. B., Falabella, M., Colaço, H. G., Tinajero-Trejo, M., Poole, R. K., ... and Giuffrè, A.
692 (2016). The terminal oxidase cytochrome bd promotes sulfide-resistant bacterial respiration and growth.
693 *Scientific Reports* ***6:*** 23788.

694 Fossing, H., Gallardoi, V., Jorgensen, B., Hiittel, M., Nielsenl, L., Schulz, H. *et al.,* (1995) Concentration and
695 transport of nitrate by the mat-forming sulphur bacterium Thioploca. *Nature* **374**: 20.

696 French, C. E., Bell, J. M., and Ward, F. B. (2007). Diversity and distribution of hemerythrin-like proteins in
697 prokaryotes. *FEMS Microbiology Letters* **279**: 131-145.

Garcia, H. E., & Gordon, L. I. (1992). Oxygen solubility in seawater: Better fitting equations. *Limnology and Oceanography* **37** 1307-1312.

Garcia-Robledo, E., Padilla, C. C., Aldunate, M., Stewart, F. J., Ulloa, O., Paulmier, A., ... and Revsbech, N. P. (2017). Cryptic oxygen cycling in anoxic marine zones. *Proceedings of the National Academy of Sciences* 201619844.

Gourmelon, C., Boulegue, J., & Michard, G. (1977). Oxydation partielle de l'hydrogène sulfuré en phase aqueuse. *CR Acad Sci Paris* **284:** 269-272.

Halm, H., Musat, N., Lam, P., Langlois, R., Musat, F., Peduzzi, S. *et al.,* (2009) Co-occurrence of denitrification and nitrogen fixation in a meromictic lake, Lake Cadagno (Switzerland). *Environmental Microbiology* **11**: 1945-1958.

Hoang, D. T., Chernomor, O., von Haeseler, A., Minh, B. Q., & Vinh, L. S. (2017). UFBoot2: improving the ultrafast bootstrap approximation. Molecular Biology and Evolution **35:** 518-522.

Holtappels, M., Tiano, L., Kalvelage, T., Lavik, G., Revsbech, N. P., & Kuypers, M. M. (2014). Aquatic respiration rate measurements at low oxygen concentrations. *PLoS One* **9:** e89369.

Imhoff, J. F., Süling, J., and Petri, R. (1998). Phylogenetic relationships among the Chromatiaceae, their taxonomic reclassification and description of the new genera *Allochromatium*, *Halochromatium*, *Isochromatium*, *Marichromatium*, *Thiococcus*, *Thiohalocapsa* and *Thermochromatium*. *International Journal of Systematic and Evolutionary Microbiology* **48**: 1129-1143.

Janz, G., Downey Jr, J., Roduner, E., Wasilczyk, G., Coutts, J., and Eluard, A. (1976) Raman studies of sulfur-containing anions in inorganic polysulfides. Sodium polysulfides. *Inorganic Chemistry* **15**: 1759-1763.

Jørgensen, B.B., Fossing, H., Wirsen, Chr.O., and Jannasch, H.W. (1991) Sulfide oxidation in the anoxic Black Sea chemocline. *Deep Sea Research Part A, Oceanographic Research Papers* **38**: S1083-S1103.

Jørgensen, B.B., and Gallardo, V.A. (1999) Thioploca spp.: filamentous sulfur bacteria with nitrate vacuoles. *FEMS Microbiology Ecology* **28**: 301-313.

Kallmeyer, J., Ferdelman, T.G., Weber, A., Fossing, H., and Jørgensen, B.B. (2004) A cold chromium distillation procedure for radiolabeled sulfide applied to sulfate reduction measurements. *Limnology and Oceanography Methods* **2**: 171-180.

Kampf, Chr., and Pfennig, N. (1980) Capacity of Chromatiaceae for chemotrophic growth. Specific respiration rates of Thiocystis violacea and Chromatium vinosum. *Archives of Microbiology* **127**: 125-135.

Katoh, K., Misawa, K., Kuma, K. I., & Miyata, T. (2002). MAFFT: a novel method for rapid multiple sequence alignment based on fast Fourier transform. *Nucleic Acids Research* **30:** 3059-3066.

Kirf, M.K., Dinkel, Chr., Schubert, Chr.J., and Wehrli, B. (2014) Submicromolar oxygen profiles at the oxic–anoxic boundary of temperate lakes. *Aquatic Geochemistry* **20**: 39-57.

Letunic, I., & Bork, P. (2016). Interactive tree of life (iTOL) v3: an online tool for the display and annotation of phylogenetic and other trees. Nucleic Acids Research **44**: W242-W245.

Luther, G. W., Findlay, A. J., MacDonald, D. J., Owings, S. M., Hanson, T. E., Beinart, R. A., & Girguis, P. R. (2011). Thermodynamics and kinetics of sulfide oxidation by oxygen: a look at inorganically controlled reactions and biologically mediated processes in the environment. *Frontiers in Microbiology* **2:** 62.

Ma, S., Noble, A., Butcher, D., Trouwborst, R. E., and Luther III, G. W. (2006). Removal of H2S via an iron catalytic cycle and iron sulfide precipitation in the water column of dead end tributaries. *Estuarine, Coastal and Shelf Science* **70:** 461-472.

Manske, A. K., Glaeser, J., Kuypers, M. M., and Overmann, J. (2005). Physiology and phylogeny of green sulfur bacteria forming a monospecific phototrophic assemblage at a depth of 100 meters in the Black Sea. *Applied and Environmental Microbiology* **71**: 8049-8060.

Markowitz, V.M., Chen, I.M.A., Palaniappan, K., Chu, K., Szeto, E., Grechkin, Y., Ratner, A., Jacob, B., Huang, J., Williams, P. and Huntemann, M., (2011). IMG: the integrated microbial genomes database and comparative analysis system. *Nucleic Acids Research*, *40*(D1), pp.D115-D122.

Marschall, E., Jogler, M., Henßge, U., and Overmann, J. (2010). Large-scale distribution and activity patterns of an extremely low-light-adapted population of green sulfur bacteria in the Black Sea. *Environmental Microbiology* **12:** 1348-1362.

Mas, J., and Van Gemerden, H. (1995) Storage products in purple and green sulfur bacteria. In *Anoxygenic Photosynthetic Bacteria*: Springer, pp. 973-990.

Millero, F. J. (1986). The thermodynamics and kinetics of the hydrogen sulfide system in natural waters. *Marine Chemistry*, **18:** 121-147.

Millero, F. J., Hubinger, S., Fernandez, M., & Garnett, S. (1987). Oxidation of H_2S in seawater as a function of temperature, pH, and ionic strength. *Environmental Science & Technology* **21**: 439-443.

Milucka, J., Kirf, M., Lu, L., Krupke, A., Lam, P., Littmann, S. *et al.,* (2015) Methane oxidation coupled to oxygenic photosynthesis in anoxic waters. *The ISME Journal*.

Musat, N., Halm, H., Winterholler, B., Hoppe, P., Peduzzi, S., Hillion, F. *et al.,* (2008) A single-cell view on the ecophysiology of anaerobic phototrophic bacteria. *Proceedings of the National Academy of Sciences* **105**: 17861-17866.

Overmann, J., Cypionka, H., and Pfennig, N. (1992). An extremely low-light adapted phototrophic sulfur bacterium from the Black Sea. *Limnology and Oceanography* **37**: 150-155.

Overmann, J. (1997) Mahoney Lake: a case study of the ecological significance of phototrophic sulfur bacteria. In *Advances in Microbial Ecology*: Springer, pp. 251-288.

Parks DH, Imelfort M, Skennerton CT, Hugenholtz P, Tyson GW. 2014. Assessing the quality of microbial genomes recovered from isolates, single cells, and metagenomes. *Genome Research* **25**: 1043-1055

Peduzzi, S., Tonolla, M., & Hahn, D. (2003). Vertical distribution of sulfate-reducing bacteria in the chemocline of Lake Cadagno, Switzerland, over an annual cycle. *Aquatic Microbial Ecology* **30:** 295-302.

Peng, Y., Leung, H.Chr., Yiu, S.-M., and Chin, F.Y. (2012) IDBA-UD: a de novo assembler for single-cell and metagenomic sequencing data with highly uneven depth. *Bioinformatics* **28**: 1420-1428.

Pfeffer, Chr., Larsen, S., Song, J., Dong, M., Besenbacher, F., Meyer, R.L. *et al.,* (2012) Filamentous bacteria transport electrons over centimetre distances. *Nature* **491**: 218-221.

Pfennig, N. (1975). The phototrophic bacteria and their role in the sulfur cycle. *Plant and Soil*, *43*(1), 1-16.

Pfennig, N., Höfling, K.-H., and Kusmierz, H. (1968) *Chromatium okenii (Thiorhodaceae)-Biokonvektion, aero-und phototaktisches Verhalten*: IWF.

Polerecky, L., Adam, B., Milucka, J., Musat, N., Vagner, T., and Kuypers, M.M. (2012) Look@ NanoSIMS–a tool for the analysis of nanoSIMS data in environmental microbiology. *Environmental Microbiology* **14**: 1009-1023.

Posth, N. R., Bristow, L. A., Cox, R. P., Habicht, K. S., Danza, F., Tonolla, M., ... and Canfield, D. E. (2017). Carbon isotope fractionation by anoxygenic phototrophic bacteria in euxinic Lake Cadagno. *Geobiology* **15**: 798-816.

Prange, A., Arzberger, I., Engemann, Chr., Modrow, H., Schumann, O., Trüper, H.G. *et al.,* (1999). *In situ* analysis of sulfur in the sulfur globules of phototrophic sulfur bacteria by X-ray absorption near edge spectroscopy. *Biochimica et Biophysica Acta (BBA)-General Subjects* **1428**: 446-454.

Schwedt, A., Kreutzmann, A. C., Polerecky, L., and Schulz-Vogt, H. N. (2012). Sulfur respiration in a marine chemolithoautotrophic Beggiatoa strain. *Frontiers in Microbiology*, *2*, 276.

Socrates, G. (2004). *Infrared and Raman Characteristic Group frequencies: Tables and Charts*: John Wiley and Sons.

Sommer, T., Danza, F., Berg, J., Sengupta, A., Constantinescu, G., Tokyay, T., Bürgmann, H., Dressler, Y., Sepúlveda Steiner, O., Schubert, C.J. and Tonolla, M. (2017). Bacteria-induced mixing in natural waters. *Geophysical Research Letters* 44: 9424-9432.

Storelli, N., Peduzzi, S., Saad, M.M., Frigaard, N.-U., Perret, X., and Tonolla, M. (2013) CO_2 assimilation in the chemocline of Lake Cadagno is dominated by a few types of phototrophic purple sulfur bacteria. *FEMS Microbiology Ecology* **84**: 421-432.

Strous, M., Kraft, B., Bisdorf, R., and Tegetmeyer, H. (2012) The binning of metagenomic contigs for microbial physiology of mixed cultures. *Frontiers in Microbiology* **3**: 410.

Tonolla, M., Demarta, A., Peduzzi, R., and Hahn, D. (1999) In situ analysis of phototrophic sulfur bacteria in the chemocline of meromictic Lake Cadagno (Switzerland). *Applied and Environmental Microbiology* **65**: 1325-1330.

Tonolla, M., Peduzzi, S., Demarta, A., Peduzzi, R., and Dittmar, H. A. H. N. (2004). Phototropic sulfur and sulfate-reducing bacteria in the chemocline of meromictic Lake Cadagno, Switzerland. *Journal of Limnology* **63:** 161-170.

Tonolla, M., Peduzzi, R., and Hahn, D. (2005) Long-term population dynamics of phototrophic sulfur bacteria in the chemocline of Lake Cadagno, Switzerland. *Applied and Environmental Microbiology* **71**: 3544-3550.

Trifinopoulos, J., Nguyen, L. T., von Haeseler, A., & Minh, B. Q. (2016). W-IQ-TREE: a fast online phylogenetic tool for maximum likelihood analysis. Nucleic Acids Research **44:** W232-W235.

Vaituzis, Z., and Doetsch, R. (1969) Motility tracks: technique for quantitative study of bacterial movement. *Applied Microbiology* **17**: 584-588.

Van Gemerden, H. (1968) On the ATP generation by Chromatium in darkness. *Archiv für Mikrobiologie* **64**: 118-124.

Vazquez, G., Zhang, J. Z., & Millero, F. J. (1989). Effect of metals on the rate of the oxidation of H2S in seawater. *Geophysical Research Letters* **16:** 1363-1366.

Verity, P. G., Robertson, C. Y., Tronzo, C. R., Andrews, M. G., Nelson, J. R., & Sieracki, M. E. (1992). Relationships between cell volume and the carbon and nitrogen content of marine photosynthetic nanoplankton. *Limnology and Oceanography* **37:** 1434-1446.

Wüest, A. (1994) Interactions in lakes: Biology as source of dominant physical forces. *Limnologica Jena* **24**: 93-104.

FIGURES

Fig 1| (A) Combined oxygen (top) and sulfide (bottom) profiles of the Lake Cadagno water column revealing the persistence of an oxygen- and sulfide- free zone over a period of 48 hours, with contour lines indicating sulfide concentrations. The bold contour lines delimiting the region with > 5 µM sulfide were used to define the chemocline in parallel profiles of *Chr. okenii* cell counts (B), particulate S^0 (C), and sulfate (D). Black dots represent sampling points for all parameters except O_2 which was measured with a microsensor mounted on a CTD probe. Shaded boxes represent dark periods between sunset at ~20:50 and sunrise at ~6:10. Time plots were interpolated from original profiles measured in August 2015 and are provided in Fig S1.

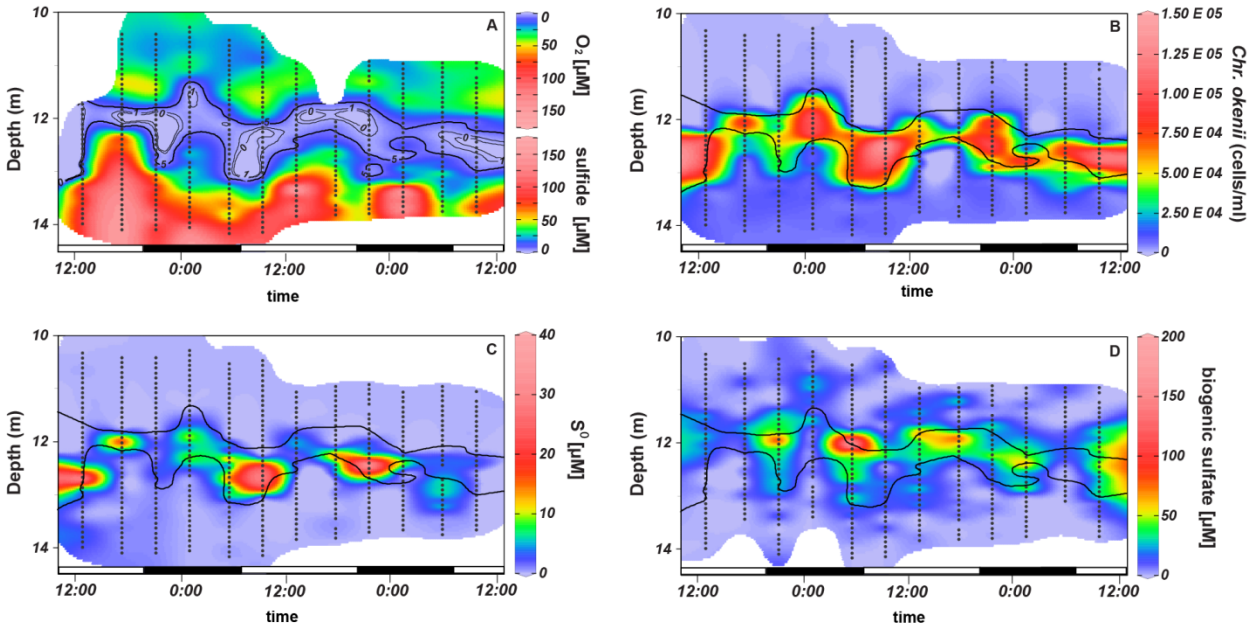

Figure 2| Representative day (A) and night (B) profiles through the chemocline illustrating glycogen and S^0 concentrations in relation to *Chr. okenii* cell numbers, oxygen, and sulfide gradients in August 2015. No oxygen data is available for the day profile. Profiles were measured at 4-h intervals over 2 day-night cycles and used to calculate chemical fluxes. (C) The consumed sulfide flux (solid line) was calculated by subtracting the residual sulfide flux (dashed line) from the total sulfide flux into the mixed layer. (D) The downwards oxygen flux into the chemocline (solid line) was used to estimate the maximum % of sulfide aerobically respired (dotted line), assuming the complete oxidation of sulfide to sulfate. Shaded regions represent dark periods.

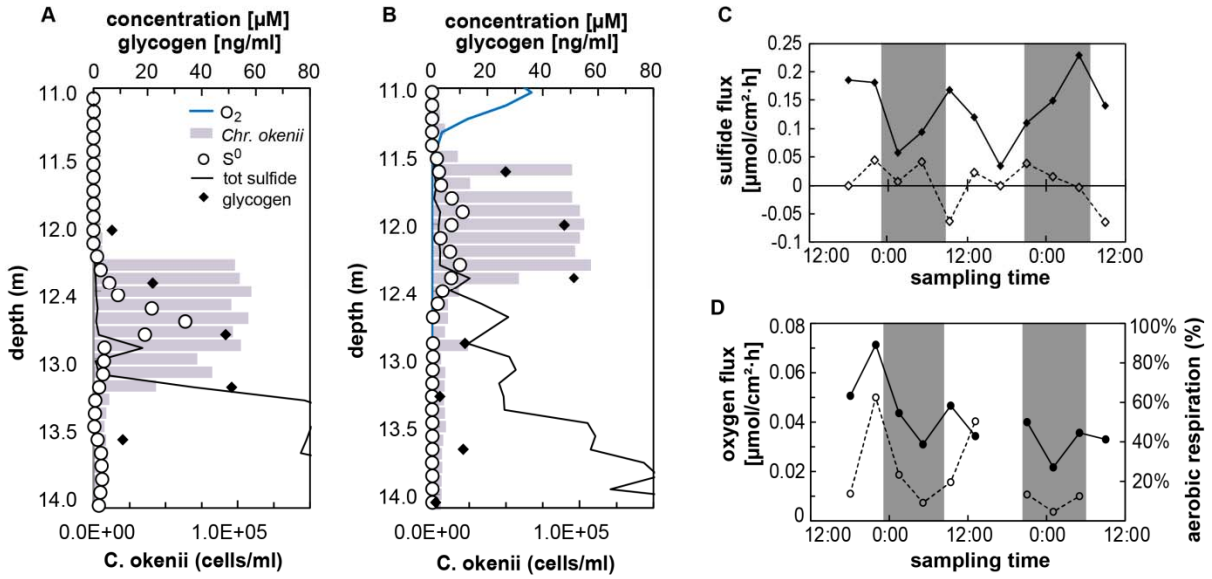

Figure 3| $^{13}CO_2$ uptake by individual *Chr. okenii* cells incubated in the dark with no O_2, 5 µM (expected) dissolved O_2, and 15 µM (expected) O_2, and in the light with no added O_2. Secondary ion images (A-C) show ratios of $^{13}C/^{12}C$. Scale bars are 3 µm and bacterial cells are outlined in white. Epifluorescence microscopy image (D) of DAPI-stained *Chr. okenii* associated with a consortium of autofluorescent algal cells enclosed within an organic sheath (dotted orange line, defined based on $^{12}C^{14}N$ image in Fig S8). White triangles denote cells identified as: *Chr* = *Chr. okenii*, *PSB* = other purple sulfur bacteria, and *np* = non-phototrophic. (E) Box-and-whisker plots showing the range and the median growth rate of *Chr. okenii* under each incubation condition calculated from ^{13}C-uptake per cell.

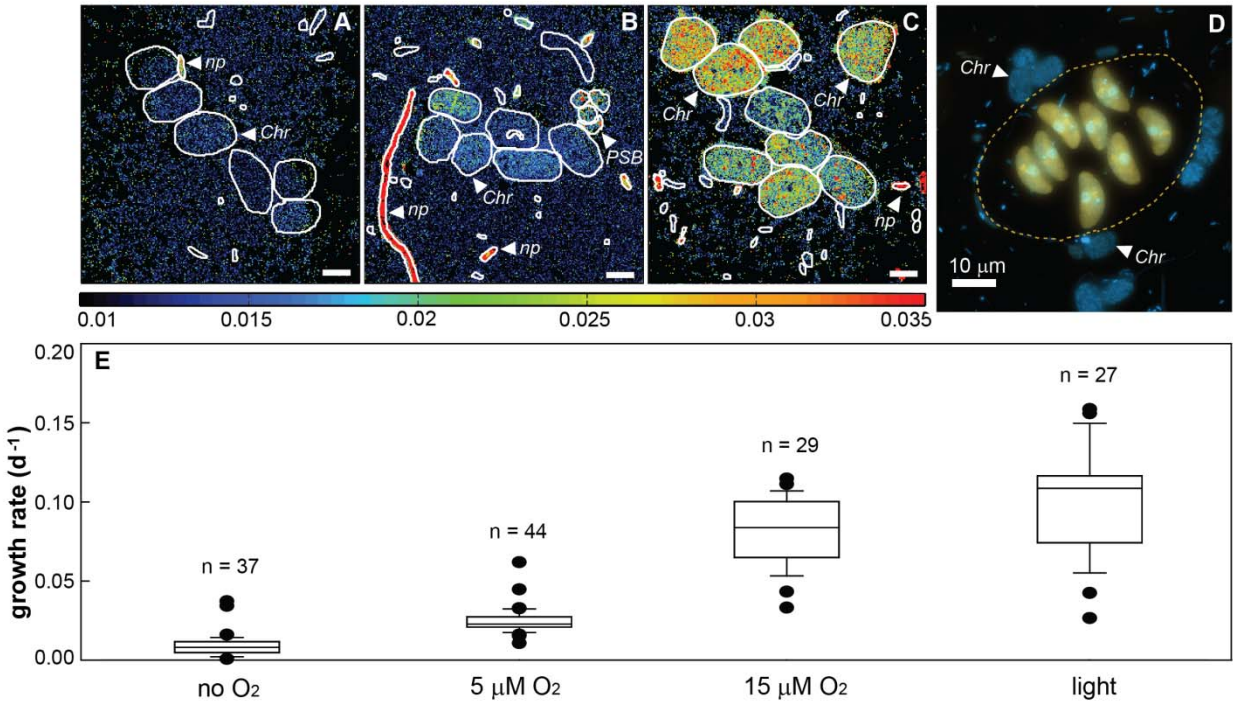

Figure 4| *Chr. okenii* cell illustration, showing the metabolic potential inferred from the metagenome-assembled genome with a particular focus on the genetic machinery implicated in photosynthesis, sulfur oxidation, aerobic metabolism, motility, glycogen and PHA storage, nitrogen fixation and transmembrane transport. The respiratory chain enzyme complexes are labeled with Roman numerals.

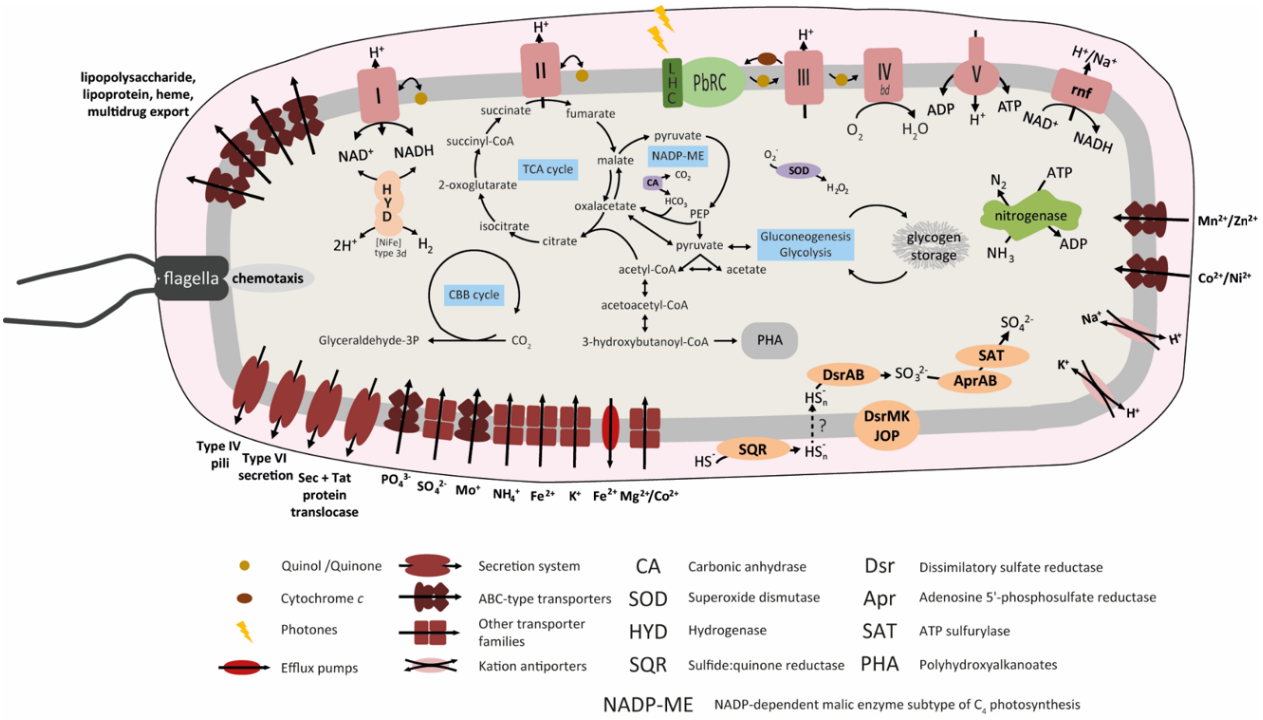
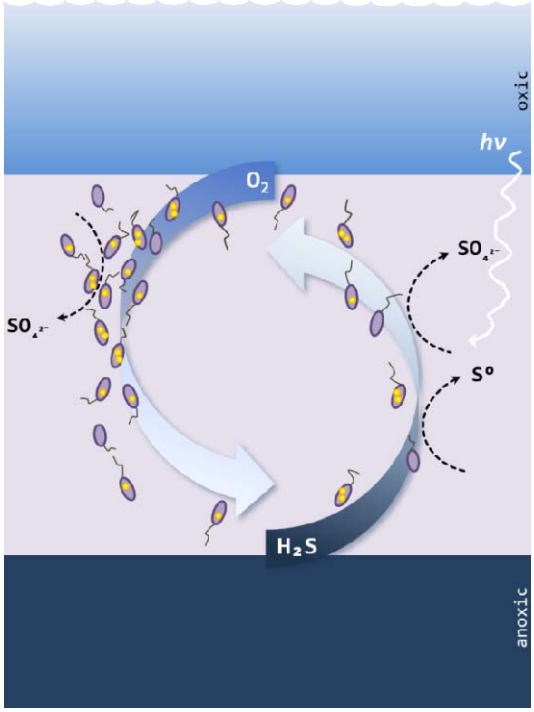
Figure 5: Schematic of phototrophic and aerobic sulfide oxidation processes in the Lake Cadagno chemocline. Convection in the chemocline may be driven by a combination of turbulence and sinking bacterial plumes, represented by the large number of descending *Chr. okenii* cells on the left. As a result, oxygen and sulfide are entrained into the chemocline and immediately consumed by purple sulfur bacteria, keeping concentrations of these compounds below detection limits. *Chr. okenii* cells, depicted with internal sulfur globules (yellow dots), are pulled in the direction of their flagellar bundle.